# ISIMA report on: Markov Chain Monte Carlo Modeling of the Tidal Stream of NGC 5466

Stephen Pardy

ISIMA Advisor: Andreas Küpper

## ABSTRACT

The Milky Way's dark matter halo remains poorly understood even in the era of high precision cosmology. Tidal streams have the unique ability to probe the potential field in the outer regions of a galaxy where the dark matter halo dominates. Although globular clusters are quite common, only a few have definite tidal tails that make them good candidates for measure the potential. In this paper we present new models for NGC 5466, a cluster with a tentative 45° tidal tail, using recently acquired radial velocity and proper motion data from bright stars in the stream. We model the tidal stream of NGC 5466 using the *streakline* code (Küpper et al. 2012) and an MCMC technique to efficiently search over a large number of models. We compare models constructed using the data of (Grillmair & Johnson 2006) with those from (Belokurov et al. 2006). Our best models constrain the Milky Way flattening parameter to be nearly 1, indicating a spherical halo, while providing new, tighter constraints for the proper motion of the cluster.

*Subject headings:* Globular Clusters, Streams

## 1. Introduction

The dark matter halo of a galaxy provides clues to its formation process and evolutionary timeline. Yet, even in the best case for studying kinematic features, i.e. our own Galaxy, the dark matter halo is poorly understood. The mass constraints vary by more than 100%, and are hampered by the fact that the halo is actually an unrelaxed structure causing the standard potential recovery methods relying on halo stars to yield biased results (Barber et al. 2013, Bonaca et al. 2014).

Dark matter halos are often modeled using a spherical NFW (Navarro et al. 1996) profile. In simulations of structure formation, dark matter halos are typically triaxial (Bullock & Zentner 2002) or have warps that make them prolate or oblate. But assessing the shapes of real halos remains very challenging. In past studies, the halo of the Milky Way has been found to be spherical, prolate, oblate and triaxial. Most of these results stem from modeling the Sagittarius dwarf stream (Law et al. 2009, Law & Majewski 2010, among others).

Tidal streams are ubiquitous in the Milky Way and stretch many degrees across the sky. These streams probe the structure of the Galaxy's potential, and since most streams are detected in the

outer halo of the Galaxy, their orbits are determined primarily by the dark matter halo (Varghese et al. 2011). Work by Lux et al. (2013) found that streams typically constrain local parameters, and lacking radial velocity data, only robustly constrain their orbital parameters. This means that we should not rely on any single stream to model the dark matter halo, but model several streams independently (or combined) to break degeneracies in model parameters.

Three candidate streams, Sagittarius, Palomar 5, and NGC 5466 have the shape, progenitor, and data necessary to facilitate high resolution modeling. Of these, Sagittarius is the most well known and has the largest amount of data, covering nearly two complete orbital loops, but is also most complicated of the streams. Proper fitting of the Sagittarius orbit is challenging and, as mentioned above, has led to very diverging results in the past (see e.g. the most recent works from Lux et al. 2013 and Gibbons et al. 2014). The work by Gibbons et al. (2014) found general agreement with previous work and a mass that falls on the low end of other authors' findings. This smaller mass Milky Way ($1 \times 10^{12} M_{\odot}$) may eliminate the "too big to fail" problem, but must be verified by modeling additional streams. Palomar 5 and NGC 5466 are the two best candidates for this. We will focus on NGC 5466 here, since we just acquired new observational data for this stream.

Belokurov et al. (2006) found evidence of a weak tidal stream extending for 2-3 deg from the NGC 5466. Grillmair & Johnson (2006) claims to trace this stream for 45 deg within the SDSS data. This stream has been modeled by a number of groups. Both Grillmair & Johnson (2006) and Lux et al. (2012) modeled the tentative 45 deg long tidal tail. This more recent work concluded that only oblate halos (with respect to the disk) and fully triaxial halos can explain an apparent upturn of the stream observed in the data (Lux et al. 2012). Using particle mesh simulations to follow faint tidal tails, Fellhauer et al. (2007) found proper motions and overdensities consistent with the Belokurov et al. (2006) tenuous tidal streams, but their result was not a unique solution as they did not attempt to explore the full parameter space of model parameters. Recently, Lux et al. (2013) showed that NGC 5466 can even constrain the triaxiality of the Milky Way halo, if there is enough phase space information.

In this work we combine existing SDSS data with new radial velocity data for NGC 5466 and its stream (section 2). We model this cluster with the efficient *streakline* method developed by (Küpper et al. 2012) (section 3.1), and apply a Markov Chain Monte Carlo (MCMC) method to search the multi-dimensional parameter space of our models, and recover the orbital properties of the cluster and bulk halo properties (section 3.3). Given our limited data, we seek to uncover only the orbital motions of the cluster, and the flattening parameter of the halo. We use parameters from recent work by Küpper et al. (in prep.) on the Palomar 5 stream to constrain the other halo parameters, and data from observational studies to try several cluster mass values. We present the results from this work in section 4 and discuss them in section 5.

## 2. Observations and Archival Data

Although originally discovered by William Herschel in the late 18th century, NGC 5466 was not known to have a tidal tail until the Sloan Digital Sky Survey (SDSS) revolutionized the study of galactic tidal streams. NGC 5466 is a northern globular cluster ∼16 kpc from the Sun with an absolute magnitude of $M_V$ = -6.96 mag (Harris 1996), and a mass to light ratio (M/L) $\sim 1-2$ giving this cluster a mass of $\sim 5-10\times10^4$ $M_\odot$, although Boyles et al. (2011) gives a higher value of $1.79\times10^5 M_\odot$. NGC 5466 has a core radius of $1.32\pm0.05'$ and a tidal radius of 20.98 $\pm0.57'$ (Lehmann & Scholz 1997); 6.1pc and 98pc at our assumed distance. Using photographic plates, Dinescu et al. (1999) estimate the proper motion of NGC 5466 to be ($\mu_\alpha cos\delta$, $\mu_\delta$) = (-4.65 $\pm$ 0.82, 0.80 $\pm$ 0.82) mas $yr^{-1}$, putting the cluster on an eccentric orbit with a 36 kpc apocenter and 4 kpc pericenter.

Belokurov et al. (2006) used a neural network to find a faint tidal tail around this long studied cluster within the SDSS data. These neural networks produce a map with probability of star in tail/probability of star in field. This can be summed to find the density of stars at each point along the sky. Their training data set consisted of $\sim$ 7000 stars in the interior of the cluster and they searched over a $6^\circ\times6^\circ$ field of view. For our modeling, we select three points by hand corresponding to the strongest features in this map (fig.1).

That same year Grillmair & Johnson (2006) observed a tentative 45° tail that is 1°.4 wide, cutoff by the SDSS field, and more tenuous than the prominent Palomar 5 stream by an order of magnitude (see figure 2). They used an optimal contrast matched-filter technique by first constructing a color-magnitude density diagram using stars within 9' from NGC 5466. They then created a weighting function by dividing this distribution by the distribution of field stars, and finally applied this weighting function to all the stars in the field. Although tenuous, Grillmair & Johnson (2006) stresses that this is not a product of dereddening, nor of a chance contamination - the feature disappears if the filter is shifted red or blueward of NGC 5466.

Adopting the proper motions from Dinescu et al. (1999), NGC 5466 would be currently near pericenter. It is stretched out and has no obvious turning points. Using a similar modeling technique than we will be applying to the NGC 5466 stream, Varghese et al. (2011) were able to fit shorter streams that show a prominent turning-point, but for streams like NGC 5466 the clusters left many halo parameters unconstrained. They concluded that line of sight velocity data is needed to constrain most halo parameters, and especially the total mass of the system.

A team lead by Jay Strader searched the region surrounding NGC 5466 using the Echelle Spectrograph on the MMT for bright member stars. They observed a total of 309 bright stars; collecting radial velocities for each. For all of these targets accurate proper motions from the SDSS data base exit, which enable us to make an efficient membership selection. We found that of these 309 stars, 63 were likely members of NGC 5466. To avoid biasing the stream modeling (which models only the stream and not the cluster itself; see below), we only use the radial velocity measurement from outside the 20.98′ (Lehmann & Scholz 1997) tidal radius of NGC 5466. This

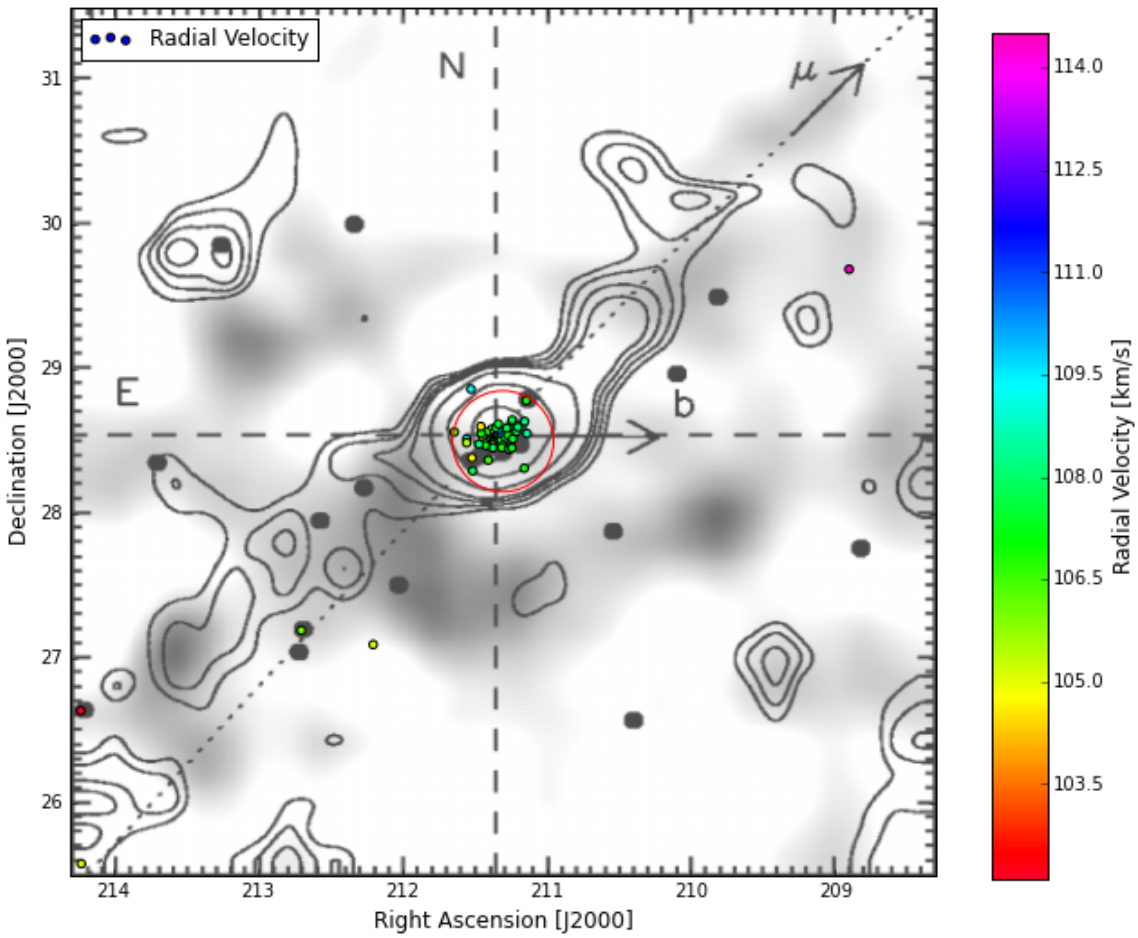


Fig. 1.— Figure adapted from Belokurov et al. (2006). The stream from Belokurov et al. (2006) overlaid with radial velocity measurements from Strader et al. (in prep.). The red circle gives the approximate tidal radius of Lehmann & Scholz (1997). The colored points are our radial velocity measurements.

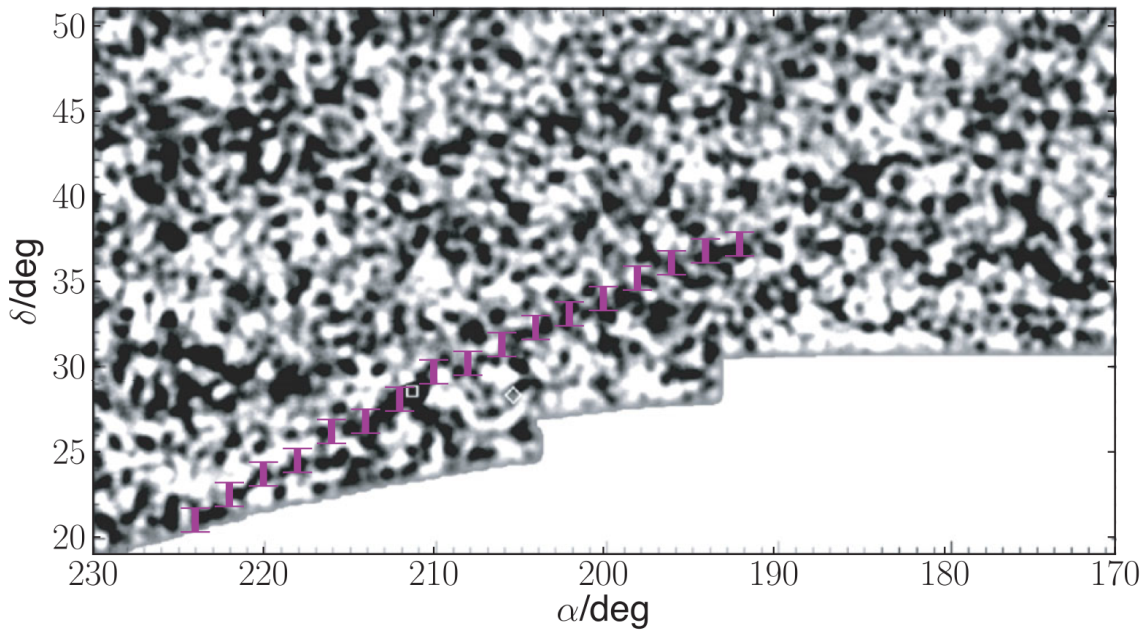


Fig. 2.— Figure adapted from Lux et al. (2012). The stream from Grillmair & Johnson (2006) with the overdensities used by Lux et al. (2012) shown as purple marks.

leaves us with six radial velocity measurements, all within $\sim 4^\circ$ of the cluster center (see fig. 1).

| $V_r$ km s$^{-1}$ | $\sigma V_r$ km s$^{-1}$ | Right Ascension Degrees (J200) | Declination Degrees (J200) | $\mu_\alpha cos(\delta)$ mas yr$^{-}$1 | $\mu_\delta$ mas yr$^{-}$1 |
|---|---|---|---|---|---|
| 109.4 | 0.1 | 211.52 | 28.86 | -4.6 | 1.6 |
| 105.1 | 1.3 | 212.20 | 27.09 | -8.0 | -2.4 |
| 106.1 | 1.0 | 212.70 | 27.19 | -3.3 | -1.6 |
| 114.5 | 0.8 | 208.91 | 29.69 | -4.2 | -0.2 |
| 102.1 | 0.7 | 214.22 | 26.64 | -6.1 | -3.0 |
| 105.2 | 1.1 | 214.22 | 25.58 | -0.2 | -0.3 |

Table 1: Radial velocity and proper motion measurements of stream stars.

## 3. Methods

### 3.1. Streaklines

A central problem in astrophysical modeling is that reproducing the proper physical phenomenon often takes such computational time as to prohibit proper parameter space searches. In

particular, with complex tidal systems such as the Sagittarius dwarf, one must either run a few expensive models to properly capture the multitude of effects, or run low resolution simulations that provide statistical power at the expense of physical accuracy.

The streakline method (Küpper et al. 2012) gives us the power to quickly and accurately model tidal streams of globular clusters like Palomar 5 and NGC 5466. Streaklines are generated by releasing test particles at a fixed time interval from the Lagrange points of the cluster-galaxy system throughout the cluster's orbit (see Sec. 3.1.1 for details). Each test particle is then evolved together with the "cluster particle" (represented by a softened point mass) as a restricted 3-body problem in the background gravitational potential of the host galaxy. The test particles do not feel any gravity from the other test particles, only from the cluster particle and the background galaxy. Hence, the typical computation times are a few seconds, to fractions of a second per model.

Küpper et al. (2012) showed that this method can accurately mimic the results from full $N$-body simulations of dissolving star clusters, which usually take hours to days of computing time. Other authors using similar methods have shown that this technique can produce unbiased results when used to infer the galactic potential (e.g. Varghese et al. 2011, Gibbons et al. 2014, Bonaca et al. 2014). One caution is that this method is only robust within the satellite's orbital apocenter (Gibbons et al. 2014). For NGC 5466 this implies a robust result within ∼40kpc.

### *3.1.1. Escape from a star cluster*

Due to two-body relaxation between stars in a star cluster, stars are constantly getting just enough energy to escape from the cluster (Heggie and Hut 2003). This process causes stars to pass by or through the two Lagrange points at slow speeds. The distance of the Lagrange points from the cluster center is usually called the tidal radius. This radius ($r_L$) is given by:

$$r_L = \left( \frac{GM_c}{\Omega_c^2 - \partial^2\Phi/\partial R_c^2} \right)^{1/3}, \tag{1}$$

(King 1962), where $G$ is the gravitational constant, $M_c$ is the mass of the cluster, $\Omega_c$ is the angular velocity of the cluster with respect to the galactic center, and $\partial^2\Phi/\partial R_c^2$ is the second derivative of the galactic potential with respect to the galactocentric radius of the cluster.

Our models release stars directly outside the Lagrange points and with angular velocities equal to those of the cluster bulk motion. We add no additional kick velocity to the stars, because we are interested in making the coldest stream possible. Adding kick velocities to mimic a wide spread of escape energies of stream stars only causes the stream to get wider, but doesn't change the overall shape of the stream (Lane et al. 2012).

We release stars at a constant rate $dt_{release}$ and follow the cluster for a given integration time $t_{int}$. In total we released $N = t_{int}/dt_{release}$ particles. In reality the cluster will lose stars at a non-constant rate as certain orbital events will cause the cluster to receive a shock from the disk

or from large features such as giant molecular clouds (Dehnen et al. 2004). These shocks compress the cluster and give all the stars a kick in energy, making those on the edges more likely to escape (Gnedin et al. 1999), while at the other end of its orbit, the cluster may expand and temporarily release less stars. However, the escape process tends to be slow for most stars (Fukushige & Heggie 2000), and work by Küpper et al. (2012) shows that it is well modeled by the constant release as an average escape rate over the orbit. That is, due to the flexing of the cluster tidal radius as it enters and leaves perigalacticon, stars that appear on the edge of the cluster, or even outside the tidal radius, may become recaptured by the cluster as it goes toward apogalacticon. To avoid recapturing test particles, we add an additional radius - the 'edge radius' - which acts as a minimum escape radius from the cluster. Küpper et al. (2012) finds that this radius shrinks with increasing orbital eccentricity, but is always larger than pericenter tidal radius, and surprisingly fits well with the observed limiting radii of globular clusters implying that there might be a physical basis. Here we set the minimum tidal radius to a small, but arbitrary value of 20 pc and increase it for an individual test particle in case it gets recaptured.

### 3.2. Galaxy Parameters

Following Küpper et al. (in prep.) and similar past works that have modeled the galactic potential as a three component model (e.g. Fellhauer et al. 2007; Koposov et al. 2010; Law & Majewski 2010; among others), we use a fixed bulge and disk component and a variable halo component as galactic background potential.

We use a Hernquist sphere (Hernquist 1990) as bulge component:

$$\Phi_{bulge} = -\frac{GM_{bulge}}{R+a}, \tag{2}$$

where $R = \sqrt{x^2+y^2+z^2}$, and we set $M_{bulge} = 3.4 \times 10^{10}\mathrm{M}_\odot$, $a = 0.7\,\mathrm{kpc}$. Moreover, we use a Miyamoto & Nagai (1975) disk model:

$$\Phi_{disk} = -\frac{GM_{disk}}{\sqrt{x^2+y^2+(b+\sqrt{z^2+c^2})^2}} \tag{3}$$

where $\mathrm{M}_{disk} = 10^{11}\mathrm{M}_\odot$, $b = 6.5\,\mathrm{kpc}$, and $c = 0.26\,\mathrm{kpc}$. These components are not the most accurate models to date, but they are simple and computationally cheap. Furthermore, studies show that models of halo streams do not rely on small variations in the bulge and disk model assumed (Varghese et al. 2011).

We model the dark matter potential as an NFW profile (Navarro et al. 1996; Binney & Tremaine 2008),

$$\Phi_{halo} = -\frac{GM_{halo}}{R_h}\frac{\ln(1+R/R_h)}{R/R_h}, \tag{4}$$

with

$$R = \sqrt{x^2 + y^2 + \frac{z^2}{q_z^2}}, \tag{5}$$

where $q_z$ is a flattening parameter, which contracts the halo along the z-axis, i.e. perpendicular to the galactic disk. We fix the parameters $R_h$ (halo scale length) and $M_{halo}$ to their values given in Küpper et al. (in prep.), as we found that our data for NGC 5466 has not enough constraining power to leave these as free parameters. Hence, we only leave $q_z$ as a free model parameter.

We use standard solar parameters with $R_\odot = 8.3$ kpc, and the Sun's circular velocity about the center of the galaxy $\vec{V}_\odot = (11.1, 258.1, 7.3)$ km s$^{-1}$(Gillessen et al. 2009; Schönrich 2012; Reid et al. 2014). With more data on NGC 5466, these parameters can also be left as free model parameters and can be included in the modeling process.

### 3.3. Markov chain Monte Carlo

In order to assess the probability of our model parameters, we use a Bayesian approach. That is, we define a likelihood, which gives us for each model a probability of detecting the observations given the respective model. This likelihood can be combined with an efficient way of searching the model parameter space like a Markov chain Monte Carlo algorithm.

A Markov chain is a system with a single current state, and many possible future states. The system goes from its current state to a future state with some finite probability, and also has a finite probability to remain at its current state. Combining this with a Monte Carlo system gives a very efficient way to search large parameter spaces. At each step, a single system (called a walker) draws random values of the input parameters and runs one simulation. The result of this simulation is a log-likelihood value:

$$LL = \sum_{j}^{N_{data}} log \left( \frac{1}{N_{model}} \sum_{i}^{N_{model}} exp^{-\frac{1}{2}\left(\frac{d_{ij}^2}{\Delta d^2}\right)} + \Delta \right). \tag{6}$$

This equation is maximized when the model parameters generates model points that lie near the $N_{data}$ observed stream fragments or radial velocity stars, respectively. This is computed by the distances $d_{ij}$ of the $i$-th model point from the $j$-th data point. The distance is calculated in the available dimensions. That is, for the stream fragments in the SDSS data, we use right ascension and declination, whereas for the radial velocity stars we use right ascension, declination, radial velocity, and proper motion (if available). Each component of the distance is weighted by its observational error, $\Delta d$. We normalize this likelihood by the number of model points ($N_{model}$) to make the likelihood value independent of the integration time, and hence number of model points. The constant $\Delta$ allows each stream fragment or radial velocity star to be an outlier, i.e. not to be part of the stream. The log-likelihood is then summed over all available data points, $N_{data}$, assuming that the data points are independent of each other.

After a model likelihood is computed, new values of the parameters are then drawn from the input distribution on a Monte Carlo basis. If the absolute value of the log-likelihood for these parameters is higher, the walker will accept this step. If the absolute value is smaller, the step will be rejected, although the walker still has a finite probability to take the step, which depends on the exact difference between the log-likelihood values. Varghese et al. (2011), Lux et al. (2012), and Bonaca et al. (2014), among others, have used this method to constrain model parameters for tidal streams.

Our models have five open parameters and six fixed parameters (see Tab. 2). We fix the present-day distance to NGC 5466 at 16 kpc based on the HST observations of (Sarajedini et al. 2007). The mass of the cluster is fixed on four separate values based on observations by (Pryor et al. 1991) and Harris 1996. These values: {5, 10, 15, 20} $\times 10^4 M_\odot$cover the range of parameter space. We lack the statistical weight to properly search over this parameter.

| Parameter | Units | Distribution | Prior | Limits |
|---|---|---|---|---|
| $\mu_\alpha cos\delta$ | mas yr$^{-1}$ | Normal | -3.55, 0.28 | -7 < $\mu_\alpha cos\delta$ < 0.1 |
| $\mu_\delta$ | mas yr$^{-1}$ | Normal | 0.11, 0.19 | -4 < $\mu_\delta$ < 5 |
| Halo Flattening $q_z$ | | Uniform | [0.5, 1.5) | 0.2 < q < 1.8 |
| Integration Time | Gyr | Uniform | [5, 4) | 0.5 < -$t_{int}$ < 10 |
| Cluster Mass | $10^4 M_\odot$ | Fixed | {5, 10, 15, 20} | N/A |
| $V_{LSR}$ | km s$^{-1}$ | Fixed | 242 | N/A |
| $R_\odot$ | kpc | Fixed | 8.3 | N/A |
| $R_h$ | kpc | Fixed | 37.9 | N/A |
| Cluster Distance | kpc | Fixed | 16 | N/A |
| Halo Mass | $M_\odot$ | Fixed | $1.58\times10^{12}$ | N/A |

Table 2: Initial parameter values (priors) and limits. Following Gibbons et al. (2014) we use brackets to denote the range of a uniform distribution, and a pair $\mu, \sigma$ to denote the mean and standard deviation around a normal distribution. The mass of the cluster is fixed at four different values.

We use 256 walkers each making 1024 steps through the parameter space for a total of 262144 simulations tested for each model.

## 4. Results

We use the median value of the posterior parameter distribution of the 262144 steps as most likely value, and the interval containing 68% above and below the median as the parameters uncertainty. Table 3 contains all of the results using the Grillmair & Johnson (2006) and those using only the Belokurov et al. (2006) data. We present the distributions for the proper motions and halo flattening parameter $q_z$ in figures 3 - 7. Each plot contains six panels, with the panels along the diagonal containing the 1D density distribution of the parameters: $\mu_\delta$, $q_z$, and $\mu_\alpha cos(\delta)$. The

panels in the bottom left triangle show the multivariate distribution of each of the parameters.

Using only the 4° data of Belokurov et al. (2006) and our new radial velocity measurements, we find a best value of the proper motions consistent with observations ($\mu_\alpha cos\delta$, $\mu_\delta$) = (-4.2 ± 6.8, 0.88 ± 5.7) mas yr$^{-1}$ Using this data produces distributions that are wide and therefore have large error values and many models that fall into unphysical regions of parameter space. Flattening parameters below 0.7 produce unphysical halos, yet our walkers consistently entered this region. Nevertheless, we find that median flattening values range between q = 0.77 ± 1.4 - 1.0 ± 1.4. There is a significant peak around a flattening value of 1, but the models do not accurate constrain this value. Most models also have very short integration times, and the distributions of parameters are not clustered around any preferred value. We present the distributions of parameters derived from this data, and using a cluster mass equal to $5 \times 10^4 M_\odot$in figure 3.

The 45° data from Grillmair & Johnson (2006) provides stronger constraints on the tidal stream. Using this data we find that the cluster proper motion is ($\mu_\alpha cos\delta$, $\mu_\delta$) = (-4.7 ± 0.90, -0.82 ± 0.69) mas yr$^{-1}$ giving the cluster a 37 kpc apocenter and 4 kpc pericenter. We are largely insensitive to flattening parameter. The median value that we q = 1.0 ± 1.1 is consistent with the value found in Küpper et al. in prep, and that found with the (Belokurov et al. 2006) data. We present the distributions of parameters in figures 4 - 7.

| Model Name (1) | $\mu_\alpha cos\delta$ mas yr$^-$1 (2) | $\mu_\delta$ mas yr$^-$1 (3) | Halo q (4) |
|---|---|---|---|
| Models based on Belokurov et al. (2006) 4° tidal stream. | | | |
| M5_4 | -4.2 ± 6.8 | 0.88 ± 5.7 | 0.86 ± 1.4 |
| M10_4 | -4.0 ± 6.5 | 0.80 ± 6.4 | 0.81 ± 1.4 |
| M15_4 | -4.1 ± 6.6 | 1.1 ± 6.2 | 1.0 ± 1.4 |
| M20_4 | -4.1 ± 6.8 | 0.83 ± 5.9 | 0.77 ± 1.4 |
| Models based on Grillmair & Johnson (2006) 45° tidal stream. | | | |
| M5_45 | -4.7 ± 0.90 | -0.82 ± 0.69 | 1.1 ± 1.0 |
| M10_45 | -4.7 ± 1.1 | -0.82 ± 1.2 | 1.0 ± 1.1 |
| M15_45 | -4.6 ± 2.6 | -0.89 ± 1.9 | 0.96 ± 1.2 |
| M20_45 | -4.5 ± 0.86 | -0.95 ± 1.8 | 1.0 ± 1.2 |

Table 3: The three open parameters of our model and their derived values from MCMC search. The model names refer to the cluster mass chosen, where the number refers to {5, 10, 15, 20}$\times 10^4 M_\odot$. The models using the data of Grillmair & Johnson (2006) have "_45" appended, while the models trying to fit the data of Belokurov et al. (2006) have "_4" appended.

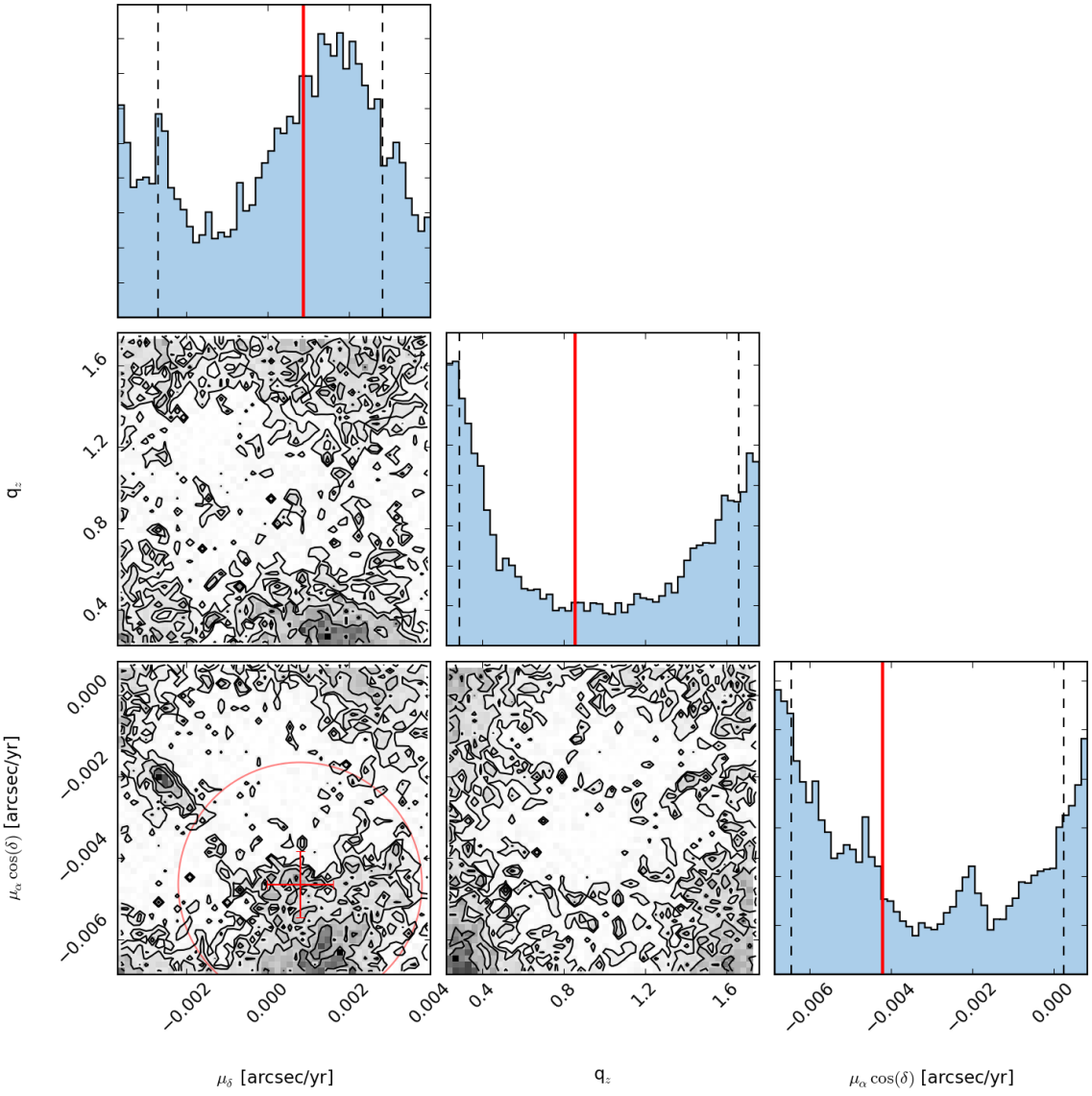


Fig. 3.— Results using the data of Belokurov et al. (2006). The panels on the diagonal show histograms of single parameters, while the grey panels in the lower left corners show the combined 2D parameter density distribution. From left to right the columns show: $\mu_\delta$, $q_z$, and $\mu_\alpha cos(\delta)$. The red cross and circle in the bottom left panel is centered on the median proper motion data. The cross shows the errors estimated from Dinescu et al. (1999), while the circle shows the more conservative error estimation from Lux et al. (2013). The red vertical line indicates the median parameter value. All panels have been scaled to show the center 90% of the data. We place weak constraints on all values, but find median proper motion values near the observation data.

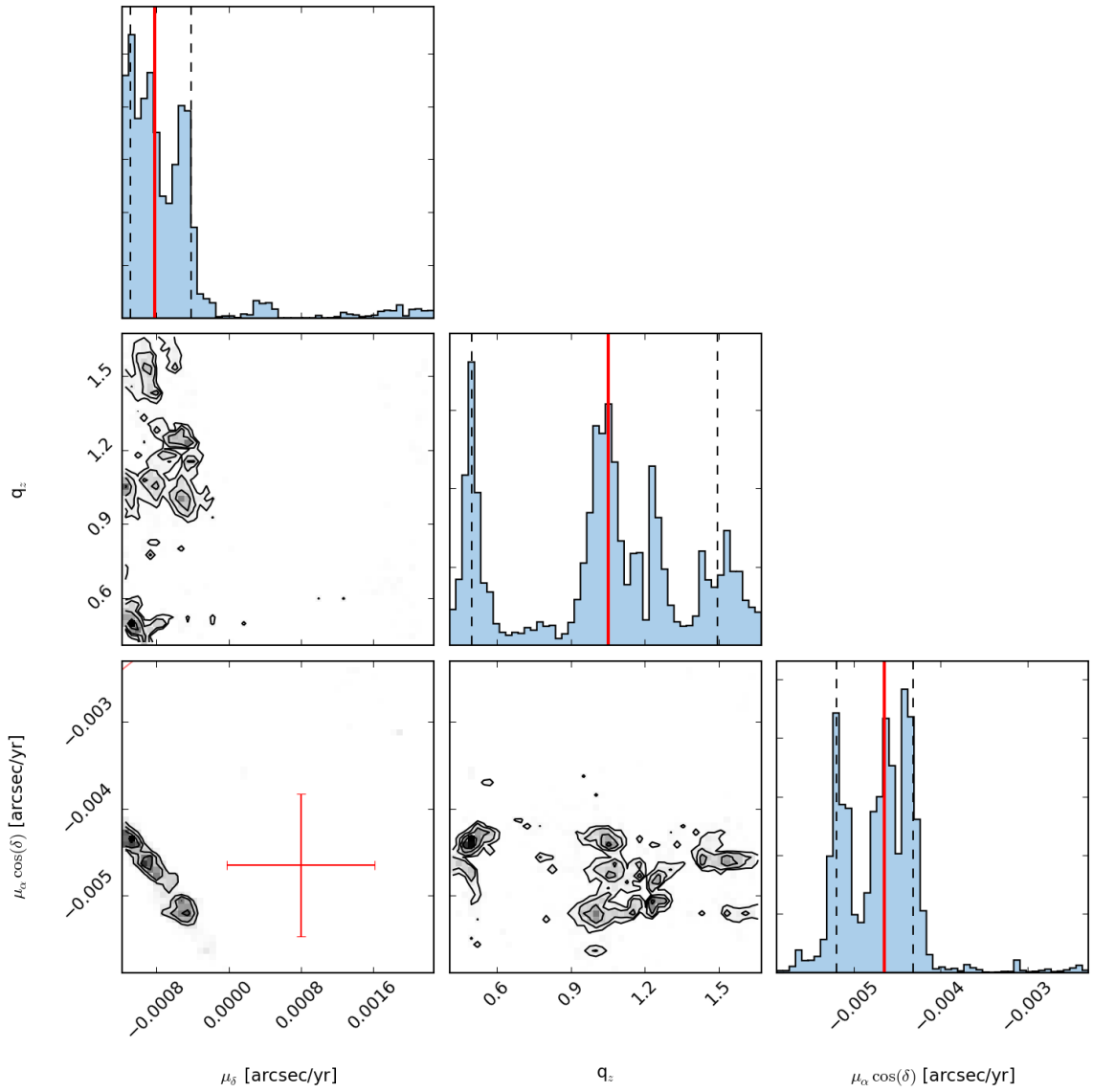


Fig. 4.— Results with the mass of NGC 5466 fixed at $5 \times 10^4 M_\odot$ using the Grillmair & Johnson (2006) data. Panels are the same as in found in figure 3. All panels have been scaled to show the center 90% of the data.

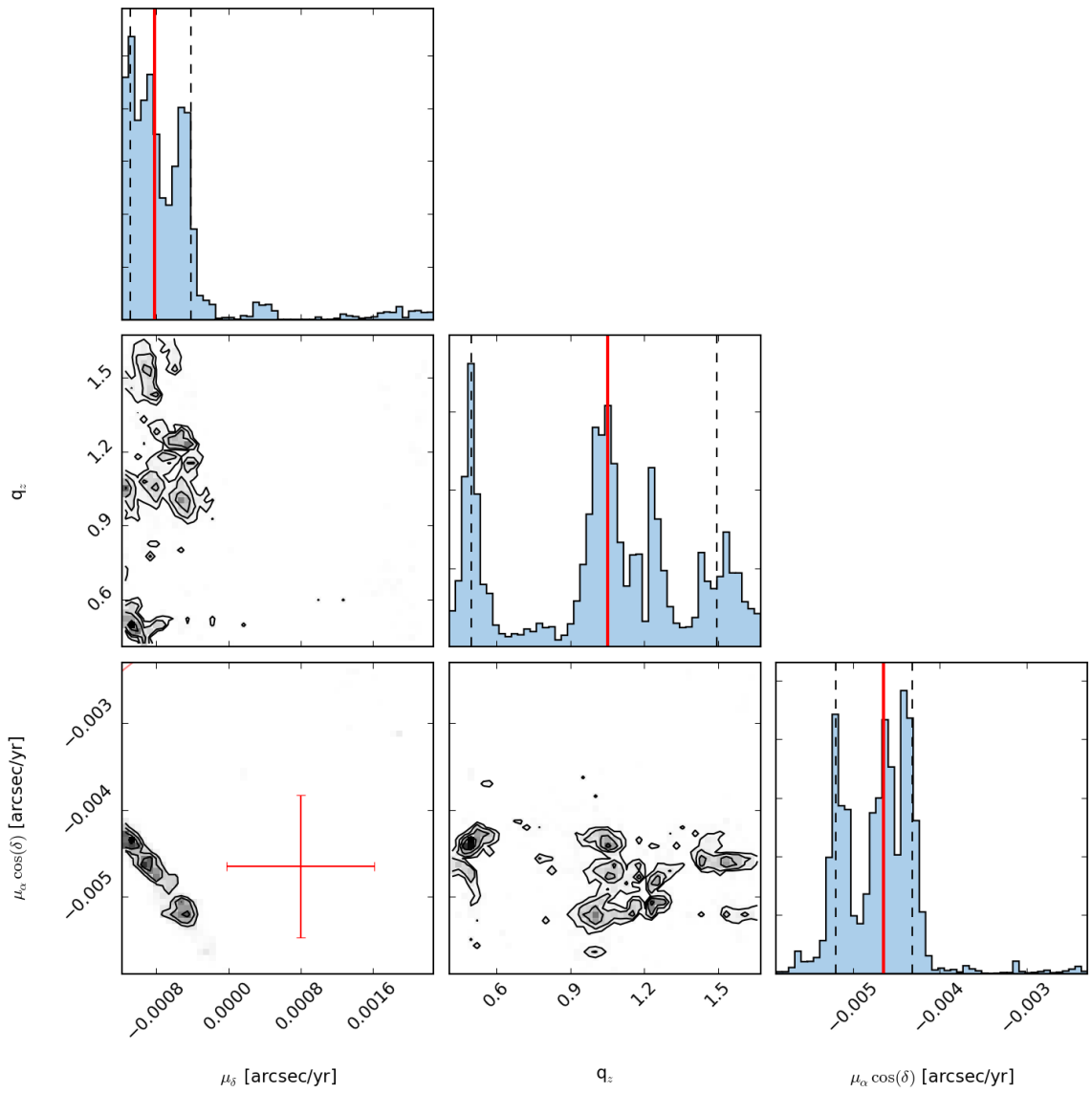


Fig. 5.— Same as in fig. 4, but with the mass fixed at $10 \times 10^4 M_\odot$. All panels have been scaled to show the center 90% of the data.

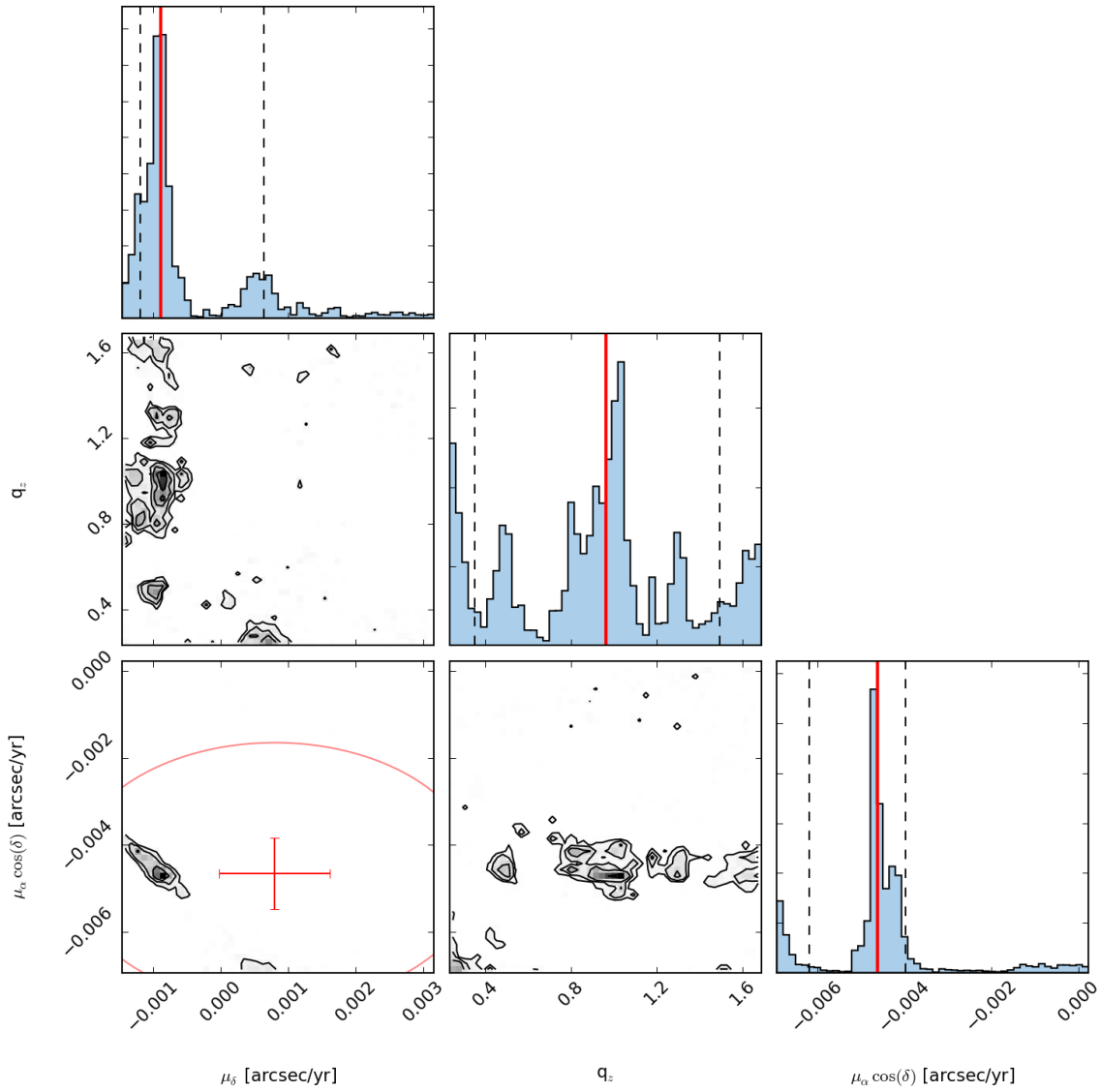


Fig. 6.— Same as in fig. 4, but with the mass fixed at $15 \times 10^4 M_\odot$. All panels have been scaled to show the center 90% of the data.

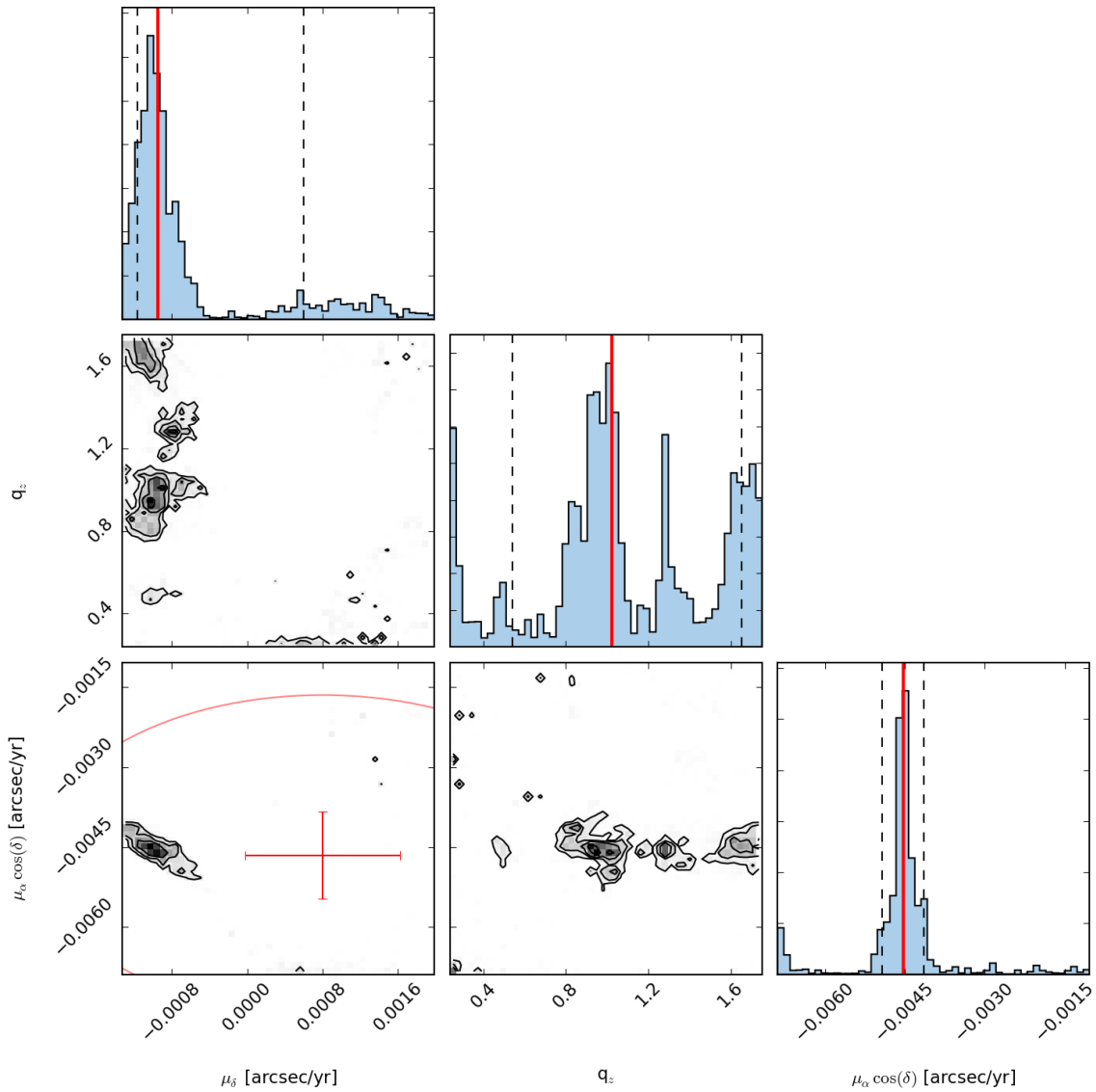


Fig. 7.— Same as in fig. 4, but with the mass fixed at $20 \times 10^4 M_\odot$. All panels have been scaled to show the center 90% of the data.

## 5. Discussion and Conclusions

The tidal stream of NGC 5466 is notoriously difficult to model, and each attempt produces comparable, but different results. Our results show that the addition of six bright radial velocity and proper motion measurements can help the effort, but we still lack data to make conclusive statements about the Milky Way's halo or NGC 5466's total mass. With the data in hand, we can accurately constrain the proper motion of the cluster, and measure the flattening of the dark matter distribution.

Further, we have tested the accuracy of the tentative 45° tidal stream found by Grillmair & Johnson (2006) by running models with and without this data. We conclude that the Belokurov et al. (2006) matches the observational evidence better, but lacks statistical power to constrain halo parameters, even when the new radial velocity measurements are included.

Küpper et al. (in prep.) measured the halo flattening parameter to be $q_z = 0.95^{+0.16}_{-0.12}$ using Palomar 5. Our flattening parameters have larger error values, but are in general agreement with theirs. Our best value, $q_z = 1.1 \pm 1.0$ implies a nearly spherical dark matter distribution in the Milky Way, in contrast to previous potential recovery papers. Nonetheless, new and tentative results show that we can also recover the proper orbital characteristics using the profile of Law & Majewski (2010). We currently lack strong enough data to say with certainty which model provides a better fit to the tidal stream of NGC 5466.

To this end, our team is currently re-analyzing the data from SDSS, and leading in an imaging and spectroscopic campaign to place stricter constraints on the tidal stream of NGC 5466. The tentative results of this work likely rule out the 45° tail. Combining this new data with the MCMC and *streakline* methods, we will make definitive statements about NGC 5466.

Our future work will combine the tidal streams of Palomar 5, NGC 5466, and the Sagittarius Dwarf into a single model. These combined models will have greater statistical power and can probe a weirder range of radii in the Milky Way. We will generalize our model by allowing density slope and triviality to act as free parameters. This will allow us to:

- Find the true dark matter density slope and resolve the "core vs. cusp" problem (e.g. Vogelsberger et al. 2014) in the Milky Way.
- Place strong constraints on the total mass of the Milky Way.
- Resolve the 3D shape of the Milky Way potential.

## REFERENCES

Barber, C., Starkenburg, E., Navarro, J. F., McConnachie, A. W., & Fattahi, A. 2013, Monthly Notices of the Royal Astronomical Society

Belokurov, V., Evans, N. W., Irwin, M. J., Hewett, P. C., & Wilkinson, M. I. 2006, ApJ

Binney, J. & Tremaine, S. 2008, Galactic Dynamics: Second Edition

Bonaca, A., Geha, M., Küpper, A. H. W., Diemand, J., Johnston, K. V., & Hogg, D. W. 2014, ApJ

Boyles, J., Lorimer, D. R., Turk, P. J., Mnatsakanov, R., Lynch, R. S., Ransom, S. M., Freire, P. C., & Belczynski, K. 2011, ApJ

Bullock, J. S. & Zentner, A. R. 2002, arXiv

Dehnen, W., Odenkirchen, M., Grebel, E. K., & Rix, H.-W. 2004, The Astronomical Journal

Dinescu, D. I., Girard, T. M., & van Altena, W. F. 1999, The Astronomical Journal

Fellhauer, M., Evans, N. W., Belokurov, V., Wilkinson, M. I., & Gilmore, G. 2007, Monthly Notices of the Royal Astronomical Society

Fukushige, T. & Heggie, D. C. 2000, Monthly Notices of the Royal Astronomical Society

Gibbons, S. L. J., Belokurov, V., & Evans, N. W. 2014, eprint arXiv:1406.2243

Gillessen, S., Eisenhauer, F., Trippe, S., Alexander, T., Genzel, R., Martins, F., & Ott, T. 2009, ApJ , 692, 1075

Gnedin, O. Y., Lee, H. M., & Ostriker, J. P. 1999, ApJ , 522, 935

Grillmair, C. J. & Johnson, R. 2006, ApJ

Hernquist, L. 1990, ApJ

King, I. 1962, The Astronomical Journal

Koposov, S. E., Rix, H.-W., & Hogg, D. W. 2010, ApJ

Küpper, A. H. W., Lane, R. R., & Heggie, D. C. 2012, Monthly Notices of the Royal Astronomical Society

Lane, R. R., Küpper, A. H. W., & Heggie, D. C. 2012, MNRAS , 423, 2845

Law, D. R. & Majewski, S. R. 2010, ApJ

Law, D. R., Majewski, S. R., & Johnston, K. V. 2009, ApJ

Lehmann, I. & Scholz, R. D. 1997, A&A

Lux, H., Read, J. I., Lake, G., & Johnston, K. V. 2012, Monthly Notices of the Royal Astronomical Society: Letters

—. 2013, Monthly Notices of the Royal Astronomical Society

Miyamoto, M. & Nagai, R. 1975, Astronomical Society of Japan

Navarro, J. F., Frenk, C. S., & White, S. D. M. 1996, ApJ

Pryor, C., McClure, R. D., Fletcher, J. M., & Hesser, J. E. 1991, The Astronomical Journal

Reid, M. J., Menten, K. M., Brunthaler, A., Zheng, X. W., Dame, T. M., Xu, Y., Wu, Y., Zhang, B., Sanna, A., Sato, M., Hachisuka, K., Choi, Y. K., Immer, K., Moscadelli, L., Rygl, K. L. J., & Bartkiewicz, A. 2014, ApJ , 783, 130

Sarajedini, A., Bedin, L. R., Chaboyer, B., Dotter, A., Siegel, M., Anderson, J., Aparicio, A., King, I., Majewski, S., Marín-Franch, A., Piotto, G., Reid, I. N., & Rosenberg, A. 2007, The Astronomical Journal

Schönrich, R. 2012, MNRAS , 427, 274

Varghese, A., Ibata, R., & Lewis, G. F. 2011, Monthly Notices of the Royal Astronomical Society

Vogelsberger, M., Zavala, J., Simpson, C., & Jenkins, A. 2014, eprint arXiv:1405.5216